

Electropolymerization Kinetics of *o*-Aminophenol and Characterization of the Obtained Polymer Films

S. M. Sayyah,¹ M. M. El-Rabiey,² S. S. Abd El-Rehim,³ R. E. Azooz¹

¹Polymer Research Laboratory, Chemistry Department, Faculty of Science (Beni-Suef Branch), Cairo University, 62514 Beni-Suef, Egypt

²Chemistry Department, Faculty of Science (Fayoum Branch), Cairo University, Fayoum, Egypt

³Chemistry Department, Faculty of Science, Ain Shams University, Cairo, Egypt

Received 1 November 2004; accepted 16 June 2005

DOI 10.1002/app.22915

Published online in Wiley InterScience (www.interscience.wiley.com).

ABSTRACT: Poly(*ortho*-aminophenol) has been synthesized electrochemically from a previously deoxygenated acid medium. The initial rate of electropolymerization reaction on platinum electrode is small and the rate law is: Rate = $k_2 [D]^{0.50} [HCl]^{1.125} [M]^{1.29}$. The apparent activation energy (E_a) was found to be 68.63 kJ mol⁻¹. The polymer films obtained have been characterized by cyclic voltammetry, X-ray diffraction, elemental analysis, TGA, scanning elec-

tron microscopy, ¹H NMR, UV-visible, and IR spectroscopy. The mechanism of the electrochemical polymerization reaction has been discussed. © 2006 Wiley Periodicals, Inc. *J Appl Polym Sci* 99: 3093–3109, 2006

Key words: electrooxidation; kinetic study; cyclic voltammetry; characterization; mechanism

INTRODUCTION

Electroactive polymers, deposited electrochemically on electrode surfaces, have received considerable attention because of possible applications of the bulk polymers themselves as well as for modified electrode surfaces, in batteries,^{1–7} electrochromic devices,^{2,8–10} microelectronic devices,¹¹ optoelectronic,¹² display devices,¹³ chemically modified electrodes,¹⁴ sensors,^{15,16} electrochemical chromatography,¹⁷ metallization,¹⁸ and as corrosion inhibitors to protect semiconductors and metals.^{18–28}

Owing to its ease of preparation, outstanding stability, and good electrical conductivity,²⁹ poly(aniline) (PAni) is one of the most common electroactive polymers for many applications. These applications are limited by the insolubility of its protonated state due to the stiffness of its backbone, and difficulty of processing by conventional methods. One of the methods that is used to overcome this problem is the polymerization of different substituted aniline derivatives.^{19,25} The obtained polymers possess higher solubility, and thus, improve solution processibility.³⁰ Common derivatives include substitution with —NH₂, —CH₃, —OCH₃, —OH, and —CH₂CH₃ groups.

The hydroxy derivative of aniline, *para*-aminophenol, has been studied.^{31,32} Its anodic oxidation gives benzoquinone as a product, but no film formation was reported. *Meta*-Aminophenol was studied chemically in acidic aqueous medium by Sayyah et al.,³³ yielding a conductive polymer with conductivity $\approx 10^{-3}$ S cm⁻¹, and electrochemically in acetonitrile³⁴ and in acidic aqueous medium.³² The obtained polymer film is nonconductive because of the presence of an activated group in this position, which leads to a double electrophilic substitution that gives a heavily crosslinked polymer structure: the crosslinked nature of this polymer prevents electronic conjugation, making it nonconductive.³⁵ On the other hand, *ortho*-aminophenol (*o*-AP), which is unstable in aqueous acidic medium particularly under the effects of light and oxygen, turning the solution yellowish after electrolysis, and brown after storing. The electrolyzed solution becomes red-brownish after some days of storing, due to the quinone-like compounds being formed.³⁵ The oxidation process of *o*-AP is complex, owing to the presence of two susceptible groups, —OH and —NH₂, which makes *o*-AP undergo hydrolysis to reactive, soluble intermediates. The electrochemical method of synthesis involves the anodic oxidation of the monomer at electrodes such as Pt,^{32,36–39} basal-plane pyrolytic graphite (BPG),⁴⁰ In-Sn oxide conducting glass (ITO),⁴⁰ glassy carbon (GC),^{32,38,41–43} Au,³² carbon paste,¹⁶ semitransparent gold,⁴⁴ and Ag.⁴⁵ The preparation of poly(*o*-aminophenol) (POAP) has been performed using cyclic voltammetry tech-

Correspondence to: S. M. Sayyah (smsayyah@hotmail.com).

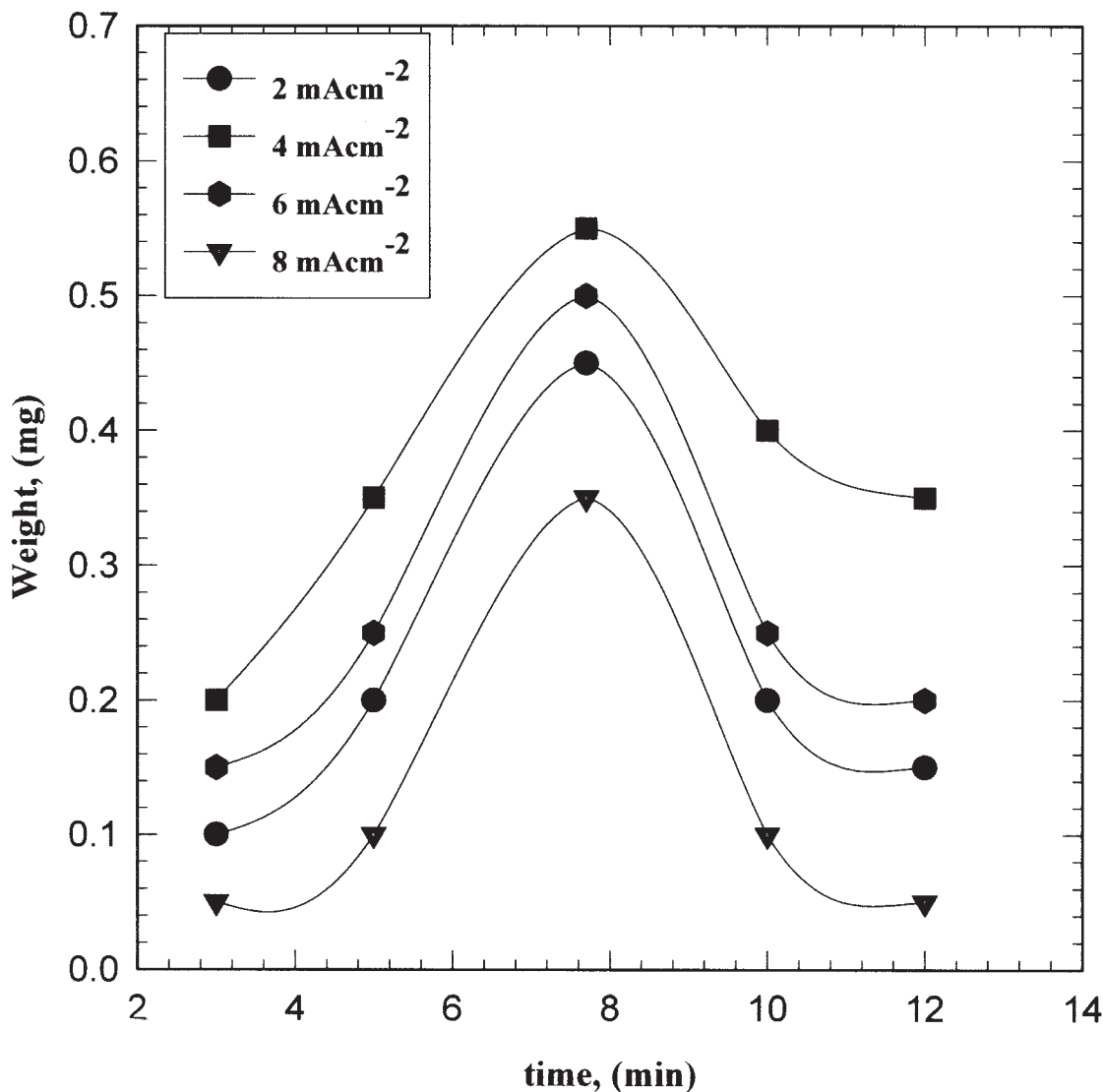


Figure 1 Yield-time curve for the effect of duration time on the anodic polymerization of *o*-AP from solution containing 0.05M monomer, 0.95M HCl, and 0.1M Na₂SO₄ at 306 K.

nique by several researchers.^{16,32,38,41–45} The polymerization was investigated at room temperature in the presence of different acids such as HClO₄,^{32,36,38,41,44,45} H₂SO₄,^{41,44} HCl,⁴³ and benzene sulfonic acid⁴⁴), fresh acetate buffer solution,¹⁶ and alkaline medium such as KOH solution.⁴⁵ Anhydrous sodium sulfate (Na₂SO₄),^{41,44} NaClO₄,^{32,36,38,40,42,44} LiClO₄,⁴² sodium benzene sulfonate,⁴⁴ etc. were used as supporting electrolytes at different concentrations. The major product in alkaline and neutral medium was identified to be 2,2'-dihydroxyazobenzene, a linear dimer formed by N–N coupling of *o*-AP radical cations. In acidic solutions, cyclic dimer 3-aminophenoxazone formed by C–N coupling of *o*-AP radical cations.

POAP is insoluble in most organic solvents (dichloromethane, ether, ethyl acetate, tetrahydrofuran, and acetone).^{32,42} The conductivity and thermodynamic

properties of the film are highly dependent on the pH of the solution.^{41,44}

In the present study, we intend to investigate the kinetics, optimum conditions, and mechanism of the electrochemical polymerization of *o*-AP in aqueous HCl solution on a platinum electrode. Also, the characterization of the obtained polymer film, using ¹H NMR, UV-visible IR, elemental analysis, TGA, and cyclic voltammetry, was performed.

EXPERIMENTAL

Materials

o-AP (WinLap, UK) was purified by recrystallizing it twice in ethyl acetate (El-Naser Pharmaceutical Chemical Company, Egypt), the pale yellow plates were

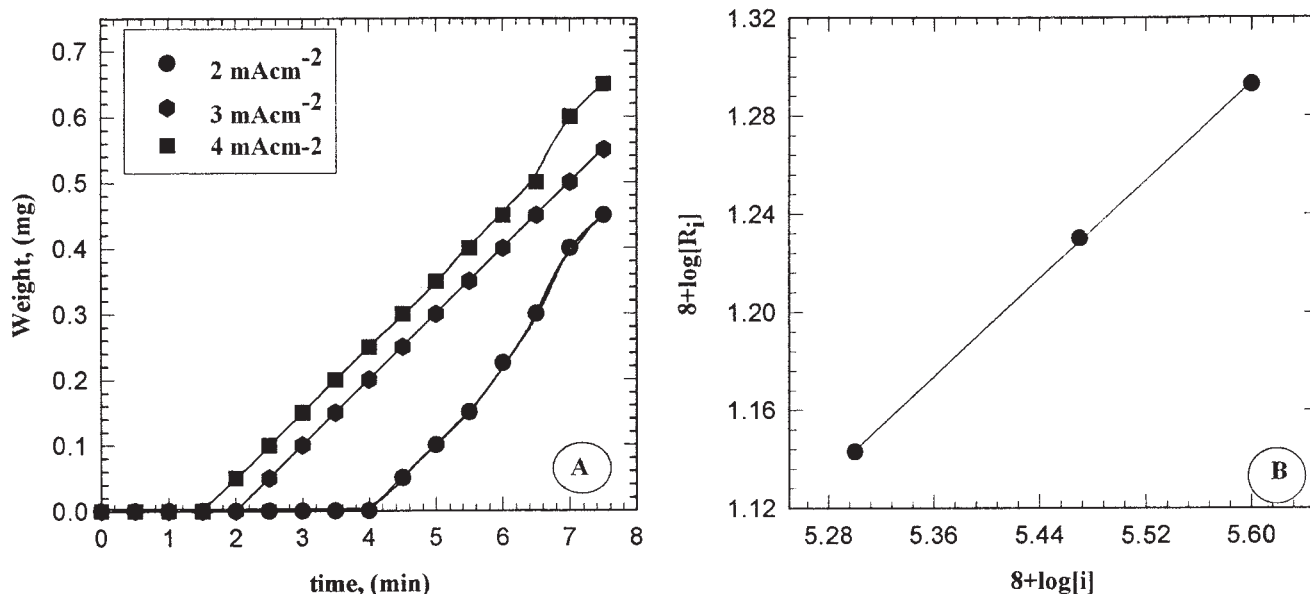


Figure 2 (A) Yield–time curve for the effect of current densities. (B) Double-logarithmic plot of initial rate of electropolymerization vs. different current density values.

then stored in a desiccator, under vacuum as described elsewhere,^{32,36,42} hydrochloric acid (Riedel-de Haën, Germany) and dimethyl formamide were provided by El-Naser Pharmaceutical Chemical Company, anhydrous sodium sulfate was provided by Merck (Darmstadt, Germany). The solutions of *o*-AP were prepared by taking a definite weight of *o*-AP and dissolving it in the supporting electrolyte solution, under nitrogen atmosphere. This process avoids air oxidation of *o*-AP, which could introduce contaminants into the film. All solutions were prepared under nitrogen atmosphere in freshly prepared double-distilled water.

Cell and electrodes

The experimental setup used consisted of a rectangular Perspex cell provided with two platinum foil parallel electrodes [dimensions: 1-cm height \times 0.5-cm width] as described previously.^{46–49} The polymerization current was supplied by a DC power supply [Thurby \sim Thandar PL 330]. Before each run, the platinum electrode (anode) was cleaned, washed with distilled water, rinsed with ethanol, dried, and weighed. The experiments were done at the required temperature \pm 1°C, using a circular, water thermostat. At the end of the experiment, the anode was withdrawn, washed with distilled water, dried, and weighed.

Electropolymerization of *o*-AP

Anodic oxidative polymerization of *o*-AP was carried out in aqueous solutions containing monomer (con-

centration range between 0.007 and 0.018M), using 0.1M Na₂SO₄ as the supporting electrolyte, and the current densities were investigated in the range between 2 and 8 mA cm⁻². Electropolymerization was carried out in hydrochloric acid solution (concentration range between 0.2 and 1.2M), at different temperatures in the range between 298 and 313 K.

Cyclic voltammetry measurements

A standard three-electrode cell was used in the cyclic voltammetry measurements, with a saturated calomel electrode (SCE) as the standard reference electrode. The auxiliary electrode was a platinum wire. The platinum working electrode was 1 \times 0.5 \times 0.05 cm³. Before each run, the working electrode was cleaned as mentioned earlier.

The electrochemical experiments were performed using an EG and G Potentiostat/Galvanostat Model 273 supplied by EG and G Princeton Applied Research. The *I*–*E* curves were recorded using computer software from the same company (Model 352 and 270/250).

IR,¹H NMR, UV–vis, and TGA

IR measurements were carried out using Shimadzu FTIR-340 Jasco spectrophotometer.

¹H NMR measurements were carried out using a Varian EM 360 L, 60-MHz NMR spectrometer. NMR signals of the electropolymerized samples were recorded in dimethyl sulphoxide, using tetramethylsilane as internal reference.

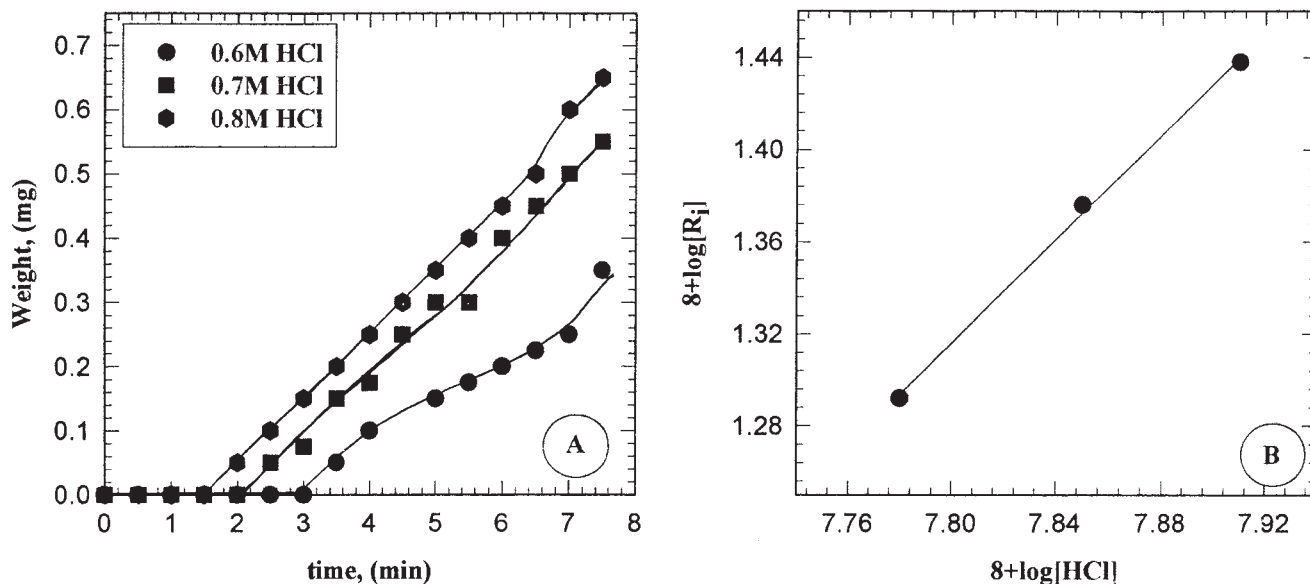


Figure 3 (A) Yield-time curve for the effect of HCl concentration. (B) Double-logarithmic plot of initial rate of electropolymerization vs. HCl concentrations.

The UV-vis adsorption spectra of the prepared polymer samples were measured using Shimadzu UV spectrophotometer (M160 PC), at room temperature in the range 200–600 nm, using dimethyl formamide as a solvent and reference.

TGA of the obtained polymer was performed using a Shimadzu DT-30 thermal analyzer (Shimadzu, Kyoto, Japan). The weight loss was measured from ambient temperature up to 500°C, at the rate of 20°C min⁻¹, to determine the degradation rate of the polymer.

Scanning electron microscopy and X-ray diffraction

Scanning electron microscopic analysis was carried out using a JSM-T20 scanning electron microscope

(JEOL, TOKYO, Japan). The X-ray diffractometer (Philips 1976 Model 1390, Netherlands) was operated under the following conditions that were kept constant for all the analysis processes: X-ray tube, Cu; scan speed, 8 deg min⁻¹; current, 30 mA; voltage, 40 kV; preset time, 10 s.

RESULTS AND DISCUSSION

Anodic oxidative electropolymerization of *o*-AP

Effect of duration time

Anodic oxidative electropolymerization of *o*-AP was studied under the influence of different plating and

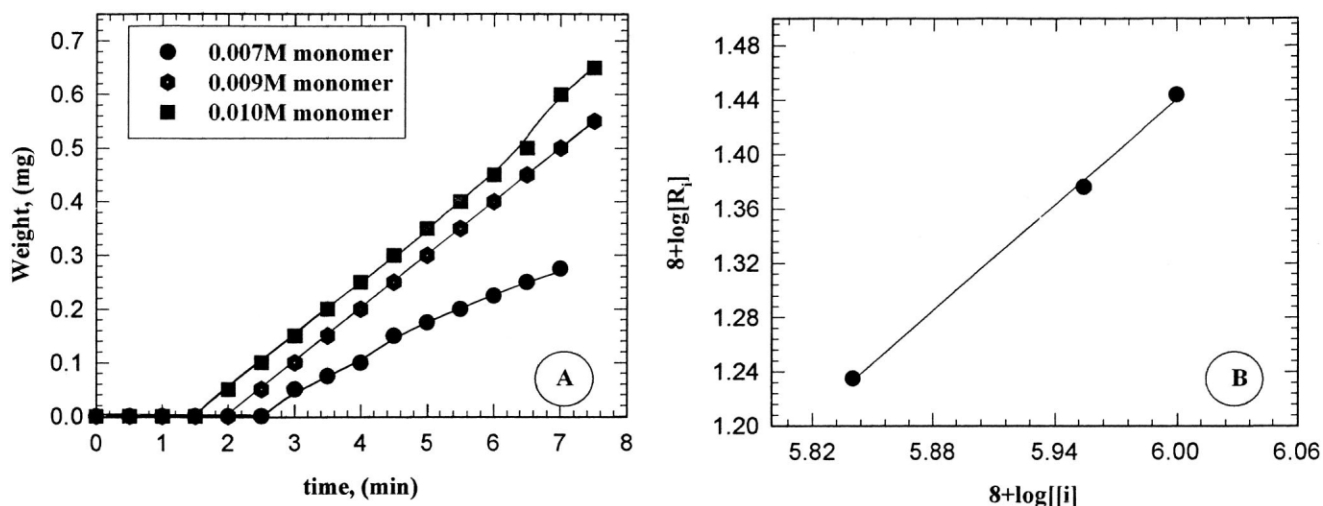


Figure 4 (A) Yield-time curve for the effect of monomer concentration. (B) Double-logarithmic plot of initial rate of electropolymerization vs. different monomer concentrations.

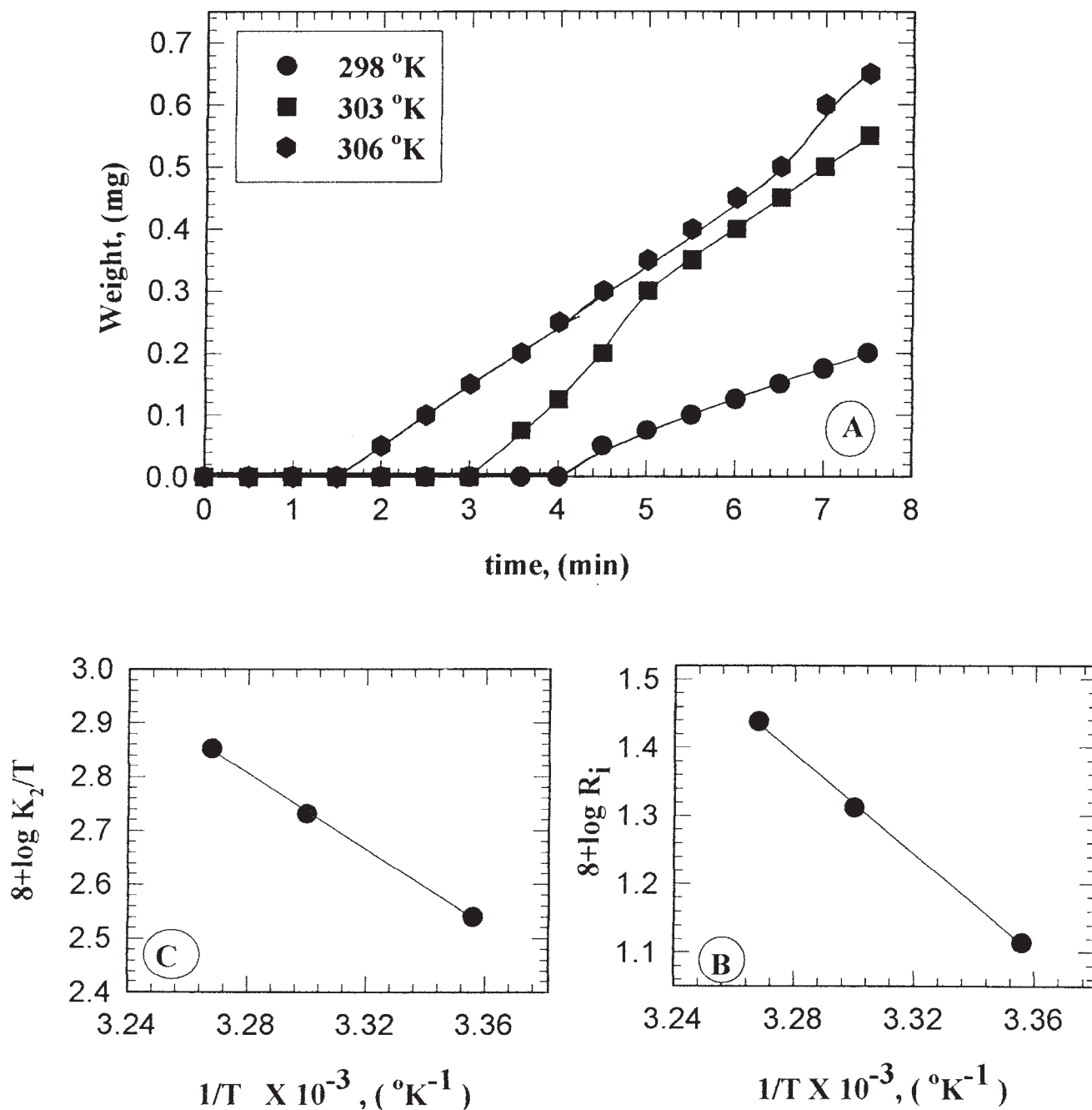


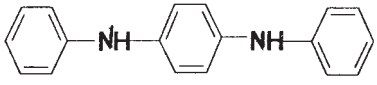
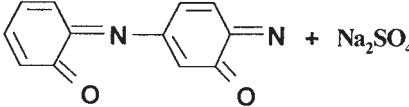
Figure 5 (A) Yield-time curve for the effect of temperature. (B) Arrhenius plot for the electropolymerization. (C) Eyring equation plot for the electropolymerization.

operating parameters. The effect of duration time on the weight of the obtained polymer films was studied with different current density values. The data reveal that, the weight of the obtained polymer increased with increase in duration time up to 7.5 min, after which it began to decrease as a result of degradation and the solubility of the polymer film from the platinum surface, in the case of all investigated values of

TABLE I
Elemental Analysis of POAP

	Calcd. (%)	Found (%)
C	51.87	50.68
H	4.76	4.9
N	10.09	9.8
Cl	10.24	10.23

TABLE II
Thermogravimetric Data of the Prepared POAP

Temperature range (°C)	Weight loss (%)		Removed molecule
	Calcd	Found	
30–100	2.53	2.10	H ₂ O
100–205	10.44	10.90	4H ₂ O
205–250	17.87	18.00	2HCl + 3(OH)
250–530	36.74	37.00	
>530	–	32.00	

the current density. The data are graphically represented in Figure 1.

Effect of current density

The effect of the applied current density on the anodic oxidative electropolymerization of *o*-AP was studied at a duration time of 7.5 min, using 0.05M monomer concentration, 0.1M Na₂SO₄ as supporting electrolyte, and 0.95M HCl at 306 K, all of which were kept constant. The data reveal that as the applied current density increases the weight of the obtained polymer film increased up to 4 mA cm⁻² and then tends to decrease. This finding implies that evolution of oxygen and chlorine takes place as a side reaction especially at high current densities. Each value of the current density used was studied at different time inter-

vals, and the yield–time curve was plotted. The data are graphically represented in Figure 2(A), from which the initial rate of electropolymerization reaction was determined. The reaction exponent, with respect to the current density, was determined from the slope of the straight line presented in Figure 2(B), and was found to be 0.50. This means that the electropolymerization with respect to the current density is a half-order reaction.

Effect of HCl concentration

Anodic oxidative electropolymerization was carried out using 0.05M monomer, 0.1M Na₂SO₄, and a current density of 4 mA cm⁻² at 306 K, for 7.5 min, all of which were kept constant. However, the concentration of HCl was varied in the range between 0.2 and 1.2M.

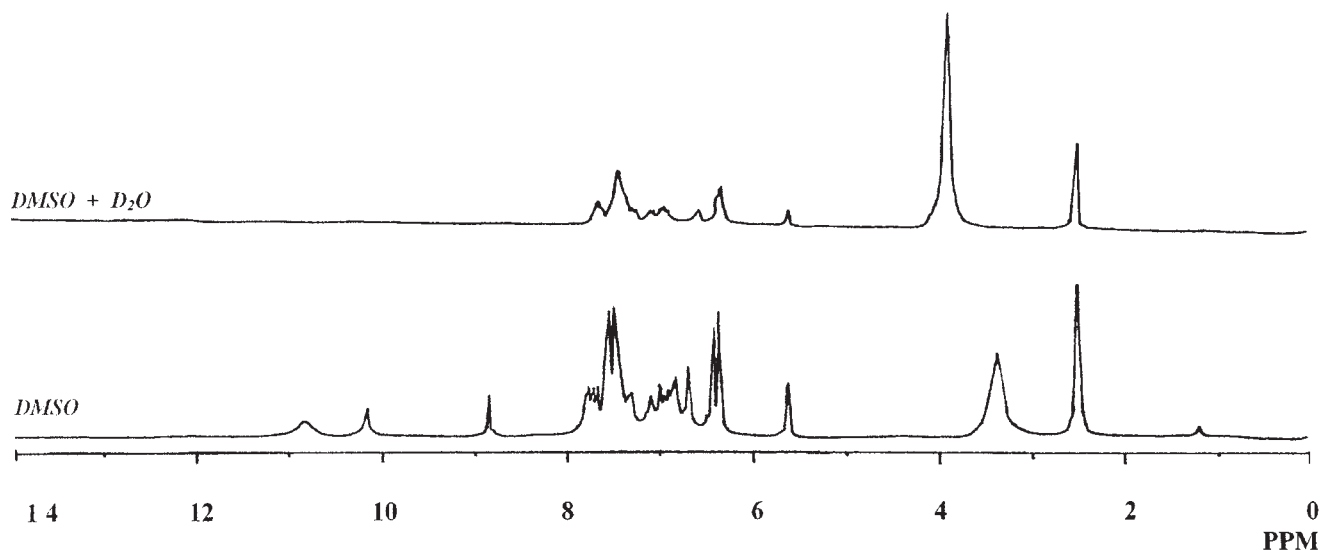


Figure 6 ¹H NMR spectrum for POAP.

TABLE III
IR Absorption Bands and Their Assignments of Both *o*-AP and POAP

Monomer	Polymer	Assignments (50)
419 ^s	–	CH wagging deformation of 1,2-disubstituted benzene ring.
447 ^s	–	
495 ^s	472 ^w	
546 ^s	554 ^m	
569 ^w	581 ^m	NH wagging deformation in aromatic amine.
712 ^s	700 ^w	
761 ^s	759 ^m	CH deformation of 1,2-disubstituted benzene ring. CH deformation of 1,4-disubstituted benzene ring.
–	799 ^m	
801 ^s	–	C-C stretching vibrations in benzene ring.
846 ^s	853 ^m	
996 ^s	–	C-O stretching vibrations.
923 ^{sh}	–	
1029 ^m	1039 ^w	C-N stretching vibrations.
1079 ^m	–	
1141 ^m	1114 ^w	NH scissoring vibrations.
1220 ^m	1183 ^s	
1267 ^m	1288 ^s	NH ₂ deformation for primary aromatic amine.
1336 ^m	1376 ^s	
1403 ^m	1418 ^s	C-N stretching vibrations for quinoide structure or combination band for protonated aromatic amine
1446 ^m	1462 ^s	
1511 ^s	1511 ^w	Stretching vibrations of C=C in benzene ring.
–	–	
1602 ^s	1602 ^s	Symmetric stretching of NH in primary aromatic amine.
–	2926 ^w	
3053 ^m	3051 ^w	Symmetric stretching of CH group.
3100 ^{sh}	3234 ^b	
3305 ^s	3334 ^b	Symmetric stretching of NH in aromatic amine.
3375 ^s	3381 ^w	
		Symmetric stretching of OH (hydrogen bonded) in phenolic compound.
		Asymmetric stretching of NH in aromatic amine.

s, strong; w, weak; b, broad; sh, shoulder; m, medium; sp, splitting.

The polymer film obtained in each experiment was weighed. The data reveal that maximum weight is obtained when 0.8M HCl was used. The effect of HCl concentration, in the range between 0.2 and 0.8M, on the electropolymerization rate was investigated. The weight of the deposited polymer film on the platinum electrode in each experiment was plotted against the duration time as shown in Figure 3(A). The initial rate of the electropolymerization reaction was calculated, and the double-logarithmic plot of the initial rate versus HCl concentration is represented in Figure 3(B). A straight line was obtained which has a slope of 1.125. This means that the electropolymerization with respect to HCl is a first-order reaction.

Effect of monomer concentration

The electropolymerization reaction was carried out by keeping all the aforementioned conditions constant at

0.8M HCl, a current density = 4 mA cm⁻², Na₂SO₄ (0.1M), reaction time (7.5 min), and temperature at 306 K, but the monomer concentrations were varied in the range between 0.007 and 0.018M. The weight of the obtained polymer film in each case was determined. From the obtained data, it was noticed that the maximum weight of the polymer film is obtained when the concentration of the monomer was 0.010M. It was also noticed that the weight of the polymer film decreased at higher monomer concentration, which means that polymer degradation may have occurred. The electropolymerization of *o*-AP was performed using different monomer concentrations in the range between 0.007 and 0.010M at different time intervals. The data are graphically represented in Figure 4(A). The initial rate of electropolymerization was calculated, and the double-logarithmic plot of the initial rate of electropolymerization versus the monomer concentration is represented in Figure 4(B). This relation gave a

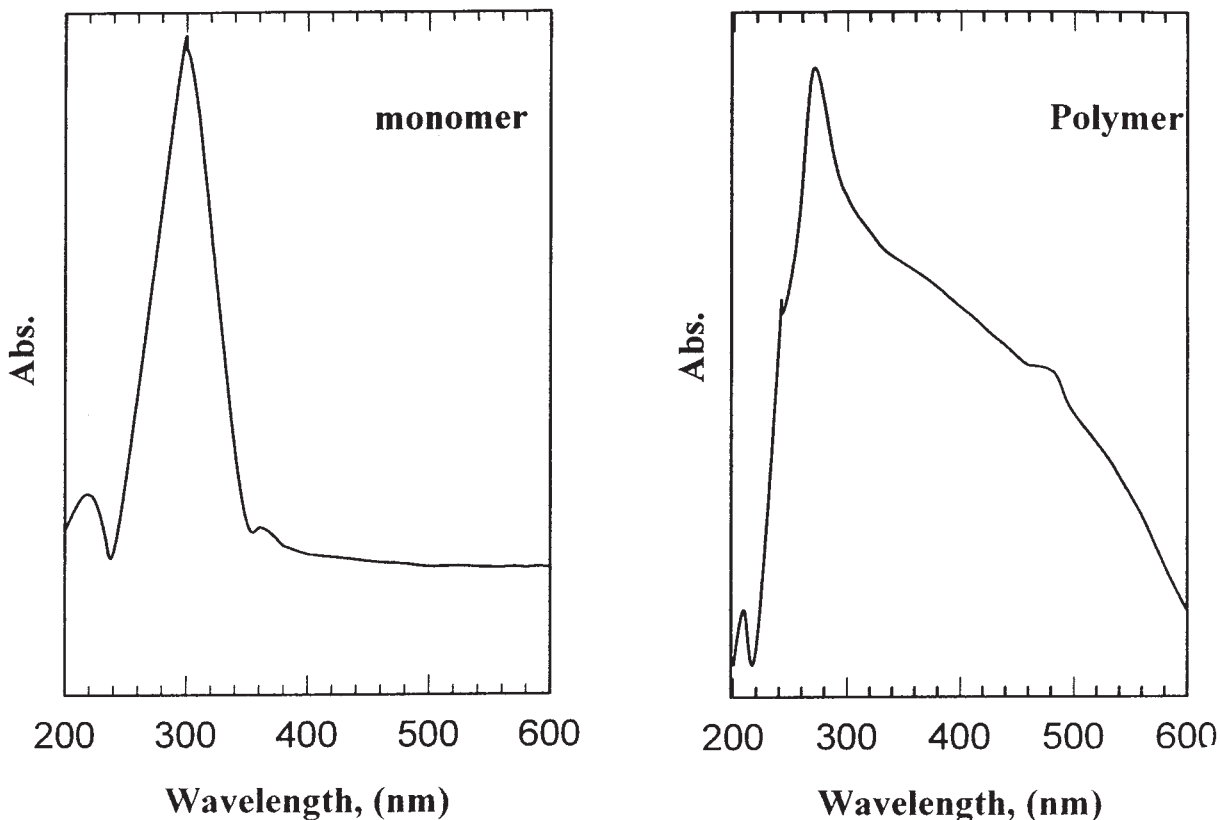


Figure 7 UV-vis spectra of 2-aminophenol monomer and its homopolymer.

straight line with a slope of 1.29, which means that the electropolymerization of *o*-AP is a first-order reaction, with respect to the monomer concentration.

Effect of temperature

Anodic oxidative electropolymerization of *o*-AP was carried out under the following constant conditions: 0.8M HCl, 0.01M monomer, 0.1M Na₂SO₄ as supporting electrolyte, current density = 4 mA cm⁻², and the duration time = 7.5 min. The reaction was carried out at different temperatures in the range between 298 and 313 K. The maximum weight of the polymer film was recorded at 306 K. It was noticed during the experiments that at temperature higher than 306 K some polymer formed in solution near the anode did not adhere at the electrode surface, which means that the adhesion of the film to the platinum electrodes decreases above 306 K. The electropolymerization of *o*-AP was carried out at different temperatures (298, 303, and 306 K) for different time intervals. At each temperature the weight of the formed polymer was plotted versus the duration time, and the yield-time curve is represented in Figure 5(A). The initial rate of electropolymerization was calculated at each investigated temperature and the logarithm of the initial rate

of electropolymerization was plotted versus 1/*T* [c.f. Figure 5(B)], which gave a straight line with a slope of -3665.3. By applying the Arrhenius equation, the apparent activation energy (*E_a*) was calculated and it was found to be 68.63 kJ mol⁻¹.

Calculation of thermodynamic parameters

The enthalpy ΔH^* and entropy ΔS^* of activation for the electropolymerization reaction can be calculated from the *k*₂ values of eq. (1). The values of *k*₂ at different temperatures were calculated, and the enthalpy (ΔH^*) and entropy (ΔS^*) of the activation associated with *k*₂ were calculated using the Eyring equation (eq. 2).

Reaction rate

$$= k_2 [\text{HCl}]^{1.125} [\text{Current density}]^{0.5} [\text{Monomer}]^{1.29} \quad (1)$$

$$k_2 = RT/Nh e^{\Delta S^*/R} e^{\Delta H^*/RT} \quad (2)$$

where *k*₂ is the rate constant, *R* is the universal gas constant, *N* is Avogadro's number, and *h* is the Planck's constant. By plotting log *k*₂/*T* vs. 1/*T* [c.f. Figure 5(C)], we obtained a linear relationship with a

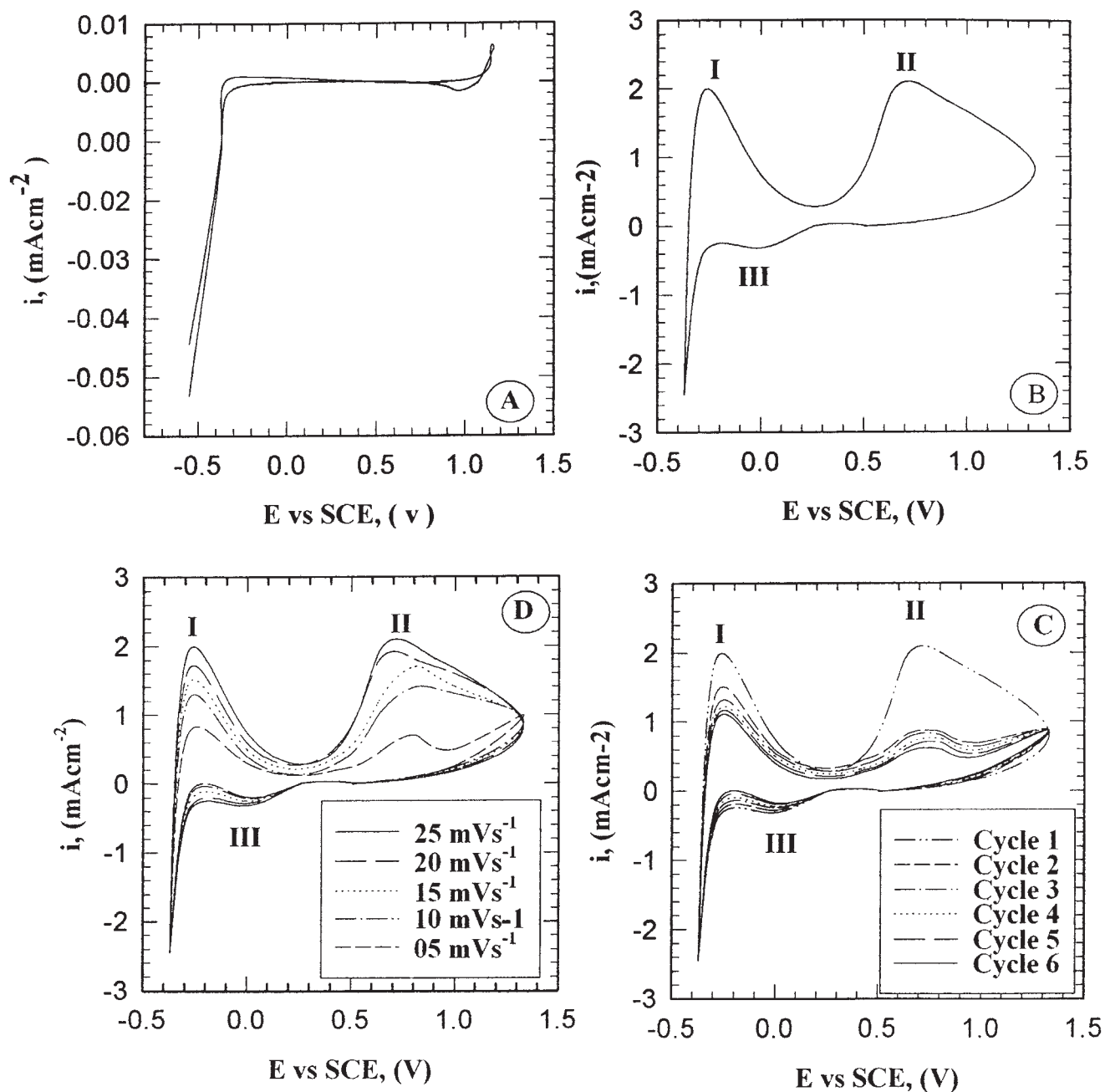


Figure 8 (A) Cyclic voltammogram curve without monomer. (B) Cyclic voltammogram curve with monomer. (C): Repetitive cycling of electropolymerization. (D) Effect of scan rate on the electropolymerization.

slope of $-\Delta H^*/2.303R$ and intercept of $\log\{(R/Nh) + \Delta S^*/2.303R\}$. From the slope and intercept, the values of ΔH^* and ΔS^* were found to be $66.03 \text{ kJ mol}^{-1}$ and $-75.16 \text{ J K}^{-1} \text{ mol}^{-1}$, respectively.

Elemental analysis and spectroscopic analysis

Elemental analytical data are given in Table I, which are in good agreement with those calculated for the suggested structure represented in Scheme 2.

The presence of five water molecules for each repeated unit is confirmed by thermogravimetric analysis. The TGA data of the prepared POAP are summarized in Table II. From the table, it is clear that there are *five* stages during thermolysis of the polymer sample.

First stage.

Includes the loss of one water molecule, in the temperature range between 30 and 100°C ; the weight loss of this step was found to be 2.10% , which is in good agreement with the calculated value (2.53%).

Second stage.

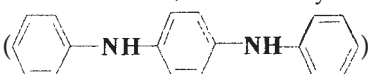
Includes the loss of four water molecules, in the temperature range between 100 and 205°C; the weight loss of this step was found to be 10.29%, which is in good agreement with the calculated value (10.44%).

Third stage.

In the temperature range between 205 and 250°C, the weight loss was found to be 18.00%, which may be attributed to the loss of two molecules of hydrochloric acid and three hydroxyl groups attached to the phenyl rings. The calculated weight loss of this stage was found to be 17.87%.

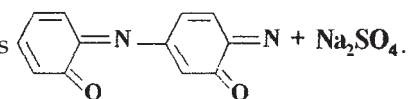
Fourth stage.

In the temperature range between 250 and 530°C, the weight loss was found to be 37.00%, which may be

attributed to the loss of  unit. The calculated weight loss was found to be 36.74%.

Fifth stage.

Above 530°C, a residual material of 32.00% was found,

which contains  + Na₂SO₄.

The ¹H NMR spectrum of the prepared POAP, which is represented in Figure 6, shows a two singlet signals at $\delta = 2.5$ and 3.5 ppm, which are attributed to solvent protons. The singlet signal appearing at $\delta = 6.4$ –7 ppm could be attributed to NH proton. The multiplet signals appearing in the region $\delta = 7$ –7.7 ppm are attributed to benzene ring protons in the polymeric structure. The singlet signals, which appear at $\delta = 7.8$ –8 ppm, may be attributed to NH₂ group protons. The singlet signal appearing at $\delta = 10.9$ ppm is attributed to the OH proton in phenolic moiety. The singlet signals appearing at $\delta = 1.2$ and 5.6 ppm are due to water of hydration. The singlet signals appearing at $\delta = 8.8$ and 10.2 ppm are due to protonated dopant molecule in the polymeric structure. The signal of OH phenolic or different types of water molecules disappeared when deuterated water was added to the sample.

The infrared absorption bands and their assignments for *o*-AP and the prepared polymer are summarized in Table III. The strong absorption band appearing at 712 cm⁻¹, in the case of monomer, appears as a weak band at 700 cm⁻¹ in the case of polymer, which could be attributed to NH wagging deformation in aromatic amine. A group of absorption bands appear in the region 801 and 1079 cm⁻¹, which in the case of monomer, appears as a medium absorption band at 853 cm⁻¹, and as a weak absorption band at 1039 cm⁻¹ in the case of polymer, which could be attributed to C—C stretching vibration in the benzene ring. Three medium absorption bands, appearing at 1141, 1220, and 1267 cm⁻¹, in the case of monomer, appear as one

weak band at 1113 cm⁻¹ and two strong bands at 1183 and 1288 cm⁻¹ in the case of polymer, which may be due to C—O stretching vibration. The strong absorption band appearing at 1511 cm⁻¹ in the case of monomer could be attributed to NH₂ deformation for primary aromatic amine. The strong absorption band at 1573 cm⁻¹ in the case of polymer, could be attributed to C—N stretching vibration of quinoid structure. Other infrared absorption bands and their assignments are summarized in Table III.

The UV–vis spectra of *o*-AP and its homopolymer (POAP) are represented in Figure 7. The spectra show the following absorption bands:

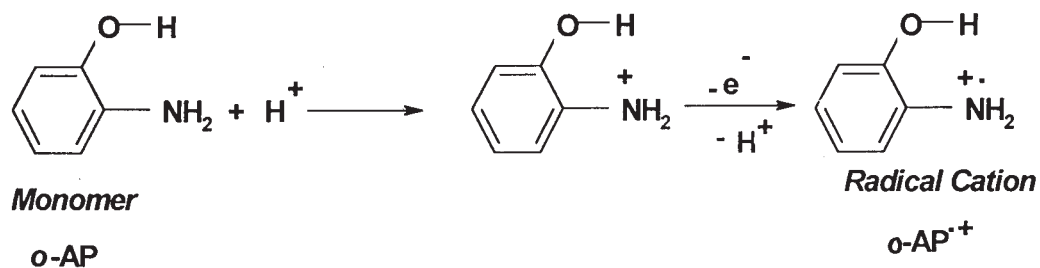
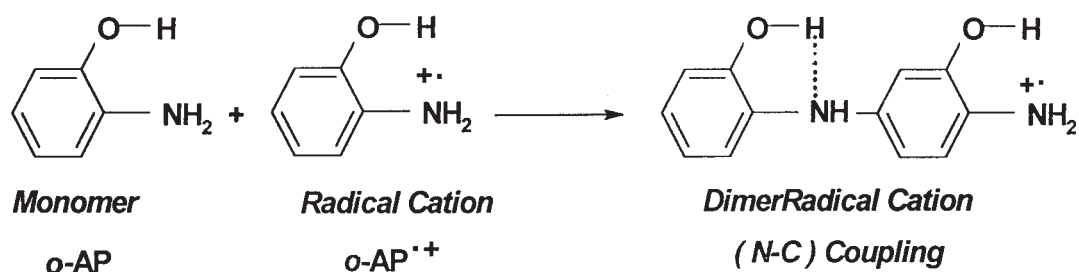
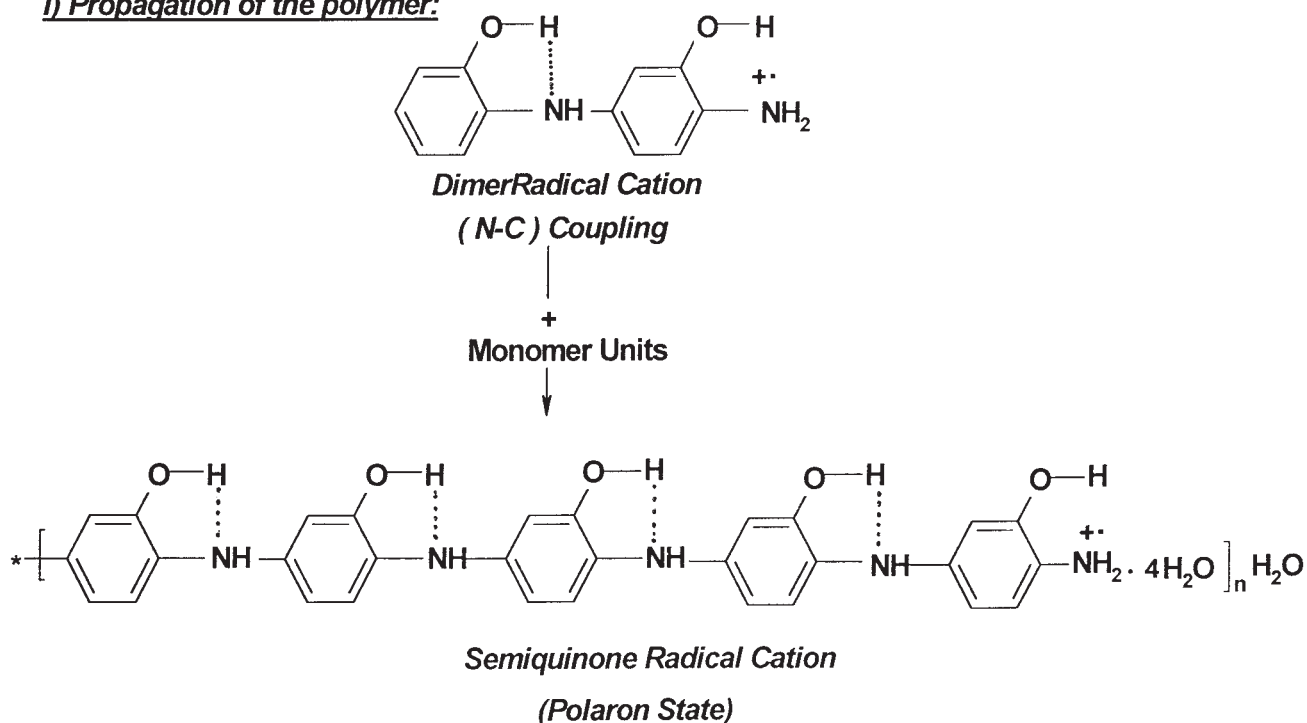
1. In the case of monomer, two absorption bands appear at $\lambda_{\max} = 220$ and 300 nm, which may be attributed to π – π^* transition (E₂ band) of the benzene ring and the β band π – π^* transition (A_{1g} to B_{2u}).
2. In the case of polymer, two absorption bands appear at lower wavelength (at $\lambda_{\max} = 210$ and 270 nm) for π – π^* transition showing a bathochromic shift. Beside these two bands, an absorption band appears in the visible region at $\lambda_{\max} = 482$ nm, which may be due to the high conjugation of the aromatic polymeric chains.

Cyclic voltammetric characterization

Cyclic voltammograms of the POAP formation on platinum electrodes from solution containing 0.8M HCl, 0.1M Na₂SO₄, at 306 K, without and with 0.01M monomer, at potentials between –400 and 1200 mV vs. SCE, with scan rate 25 mV s⁻¹, are shown in Figures 8(A) and (B), respectively.

The voltammogram in the presence of the monomer exhibits two oxidation peaks I and II that progressively developed repetitively at –300 and +810 mV vs. SCE. On the one hand, the first oxidation peak I corresponds to removing of one electron from the nitrogen atom of the amino group to give radical cation. The presence of hydroxyl group in the ortho position facilitates the oxidation process (–300 mV vs. SCE), and the formation of radical cation at low potential. The formed radical cation interacts with other monomer molecules to form dimer radical cation, followed by further reaction with monomer molecule to give trimer radical cation, and so on. Finally, the semiquinone radical cation (polaron state) is formed, which is adsorbed on the electrode surface, as shown in Scheme 1.

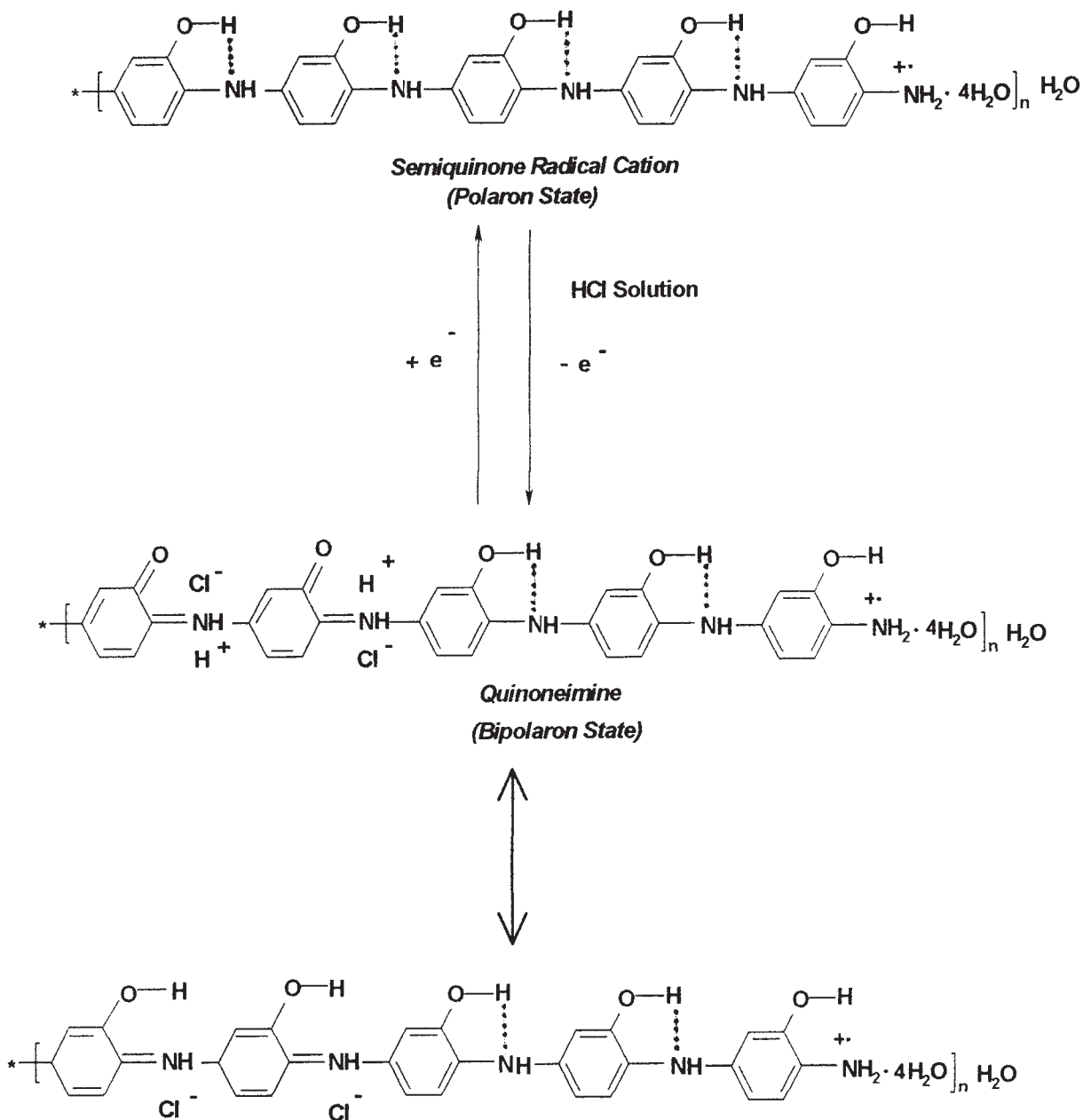
On the other hand, the second oxidation peak II, which is assigned to the oxidation of the adsorbed semiquinone radical cation (polaron state) to the quinone imine (bipolaron state),⁵¹ occurs at +810 mV vs. SCE, and is represented in Scheme 2. Therefore, the

i) Formation of radical cation:***i) Formation of dimer radical cation:******i) Propagation of the polymer:***

Scheme 1

second anodic peak is attributed to the conversion of radical cations to the fully oxidized form (quinoidal structure). However, as soon as polymerization is nucleated, a brown polymer film is rapidly observed on

the electrode surface. The potential difference between the first and the second oxidation peaks I and II is ≈ 1110 mV, and no middle peaks were observed between them, which confirm the nonexistence of deg-



Scheme 2

radation products, higher regularity, homogeneity, and adherence of the deposited film to the electrode surface.⁵¹ On reversing the potential scan from +1200 up to -400 mV, the reversing anodic current is very small, indicating the presence of adherent layer of the polymer on the electrode surface. Beyond +350 mV, the reversing cathodic scan involves a cathodic peak III. The cathodic peak III could be ascribed to the reduction of the bipolaron state to polaron state (conjugated to the second oxidation peak II). The charge involved in the cathodic peak III is smaller than that consumed in the anodic peak II, with increasing the number of cycles.

Figure 8(C) shows the effect of repetitive cycling on the formation of POAP from a solution containing 0.01M monomer, 0.8M HCl, 0.1M Na₂SO₄, at 306 K. The data reveal that the peak currents i_{pI} and i_{pII} of the two anodic peaks I and II decrease. This could be attributed to the presence of a part of the unreduced polymer film on the electrode surface; therefore, the currents of the following anodic half cycle decrease. It is possible that the stability of the deposited film is enhanced with successive cycling, and therefore, the peak currents of the cathodic and anodic peaks continue to decrease with repetitive cycling. The potential position of the redox peaks does not shift with increas-

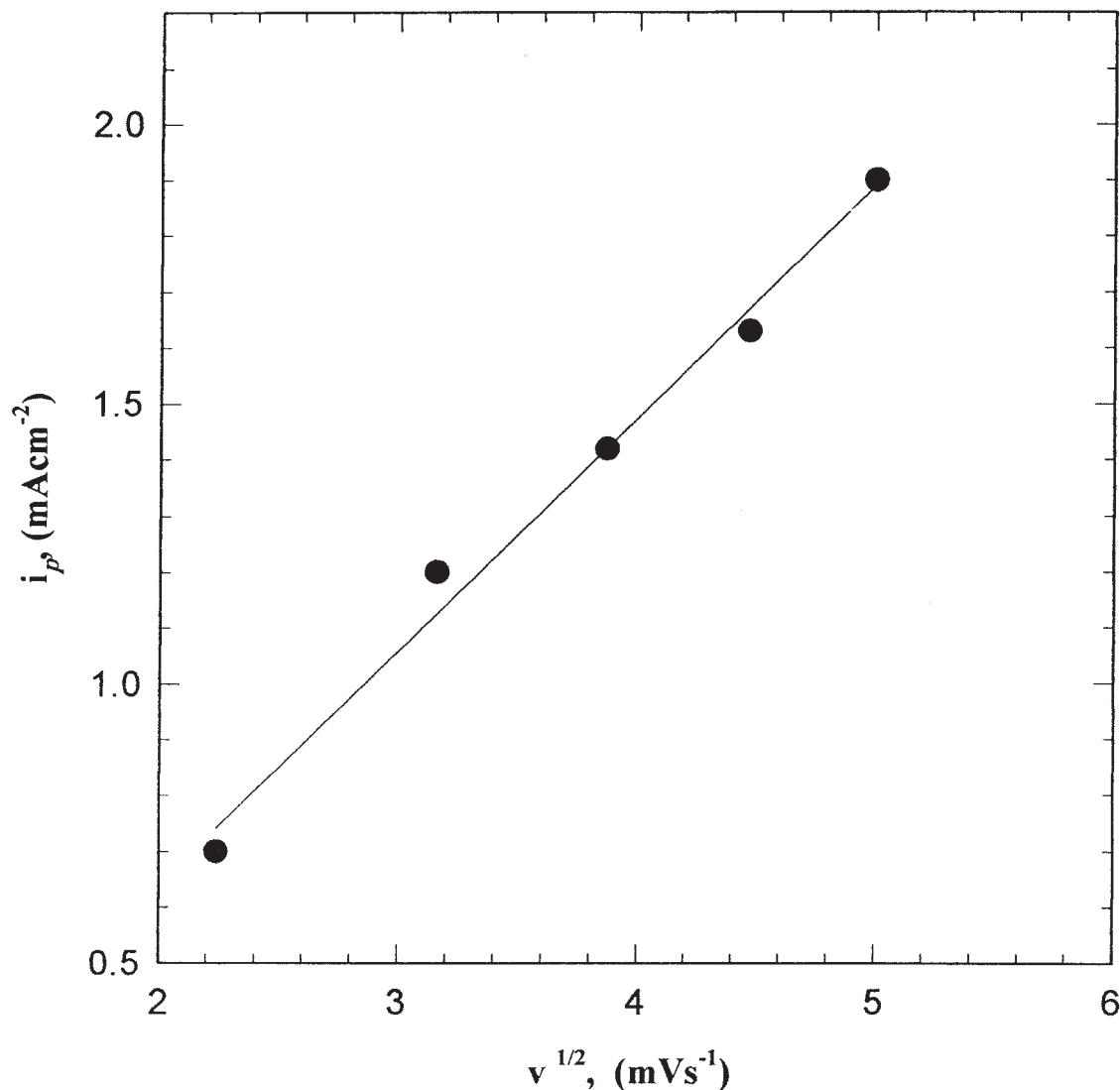


Figure 9 Relation between $v^{1/2}$ and i_p for the first anodic peak.

ing number of cycles, indicating that the reversibility of the redox reactions is independent on the polymer thickness.

Figure 8(D) shows the influence of scan rate (5–25 mV s^{-1}) on the anodic polarization curve for the electropolymerization of O-AP from a solution containing 0.01M monomer, 0.8M HCl, 0.1M Na_2SO_4 , at 306 K, on platinum electrode. The data reveal that the peak current densities i_{pI} and i_{pII} of the first and second anodic peaks, respectively, increase with increase of the scan rate, with slight decrease of the potential of the anodic peak II to more negative value. Figure 9 shows the linear dependence of the first current peak, i_{pI} , vs. $v^{1/2}$. This linear relation suggests that the electroformation of the radical cation may be described partially by a diffusion-controlled process (diffusion of reacting species to the polymer film/solution interface). It seems

that the charge of the cathodic peak III also increases, with increasing of the scan rate up to 25 mV s^{-1} .

The effect of HCl concentration, monomer concentration, and temperature on the cyclic voltammetric characteristics of the polymer film formation on platinum surface was investigated.

Figure 10(A) represents the influence of HCl concentration in the range between 0.2 and 1.0M on the electropolymerization process at 25 mV s^{-1} . The plot shows that, the peak current densities i_{pI} and i_{pII} increase with increasing HCl concentration up to 0.8M, and then starts to decrease with further increase in HCl concentration. These results are in agreement with those obtained in the kinetic study.

Figure 10(B) shows that by increasing the concentration of the monomer from 0.005 to 0.01M the anodic peak current densities i_{pI} and i_{pII} are enhanced and

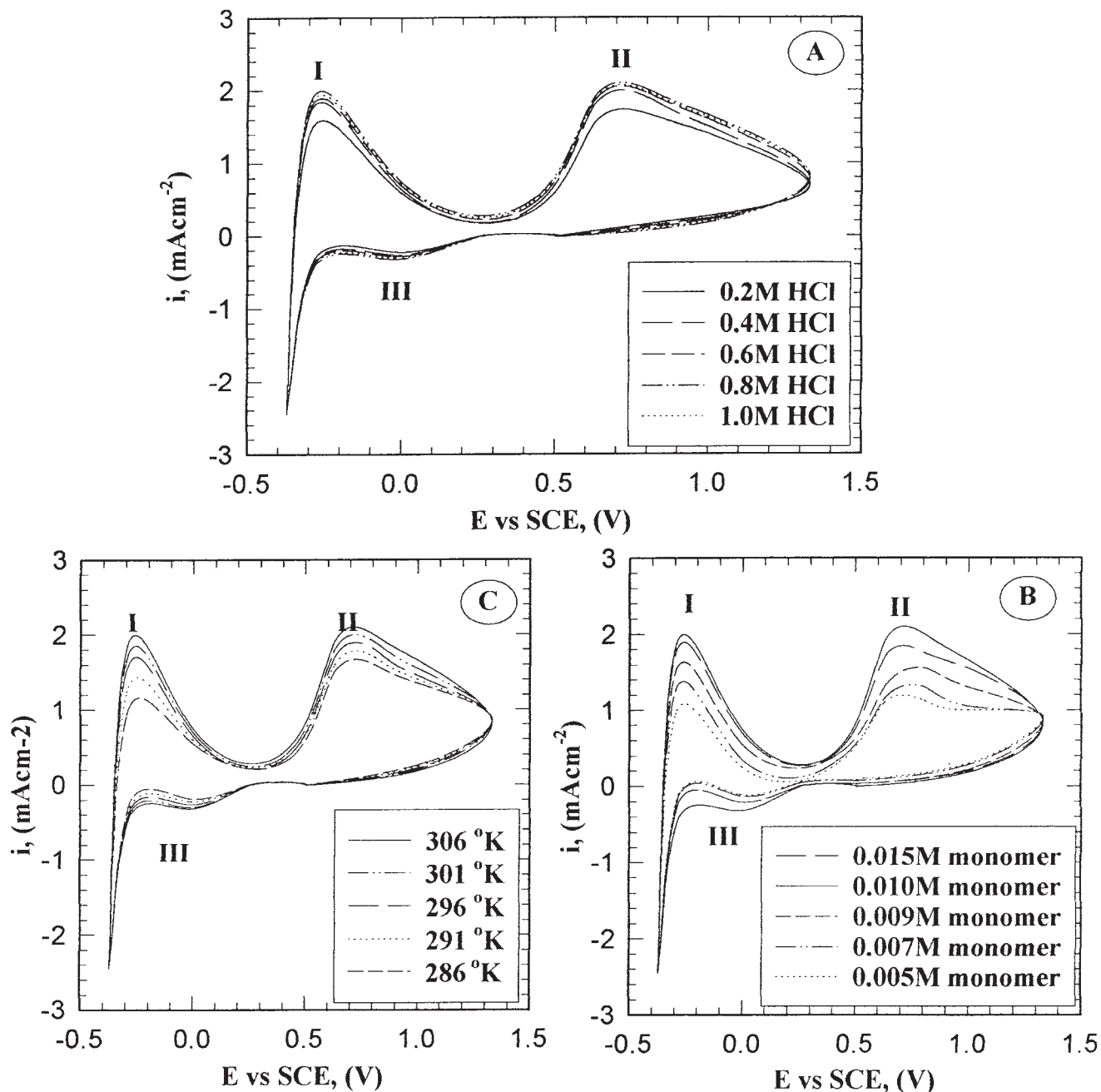


Figure 10 Cyclic voltammogram curves for the electropolymerization of *o*-AP from solution containing 0.1M Na₂SO₄: (A) effect of HCl concentration, (B) effect of monomer concentration, (C) effect of temperature.

then start to decrease. These results are in agreement with those obtained in the kinetic study.

Figure 10(C) illustrates the influence of solution temperature, from 286 to 306 K, on the cycling voltammetric response of the polymer formation. The data reveal that an increase of temperature up to 306 K results in a progressive increase of the charge included in the anodic peaks I and II and increase of the charge included in the cathodic peak III.

The electropolymerization of *o*-AP on the Pt electrode from a solution containing 0.1M Na₂SO₄, 0.01M

monomer, and 0.8M HCl was carried out. The cyclic voltammogram of the formed polymer sample on the Pt electrode in presence of the aforementioned materials and concentrations, except monomer, using different acid concentration, is represented in Figure 11. From the figure it is clear that the voltammogram shows one small oxidation peak at -200 mV vs. SCE, which could be attributed to electroactive species formed by partial degradation of the film. Also the voltammogram shows one reduction peak at +900 mV vs. SCE, which could be attributed to the reduction of the bi-

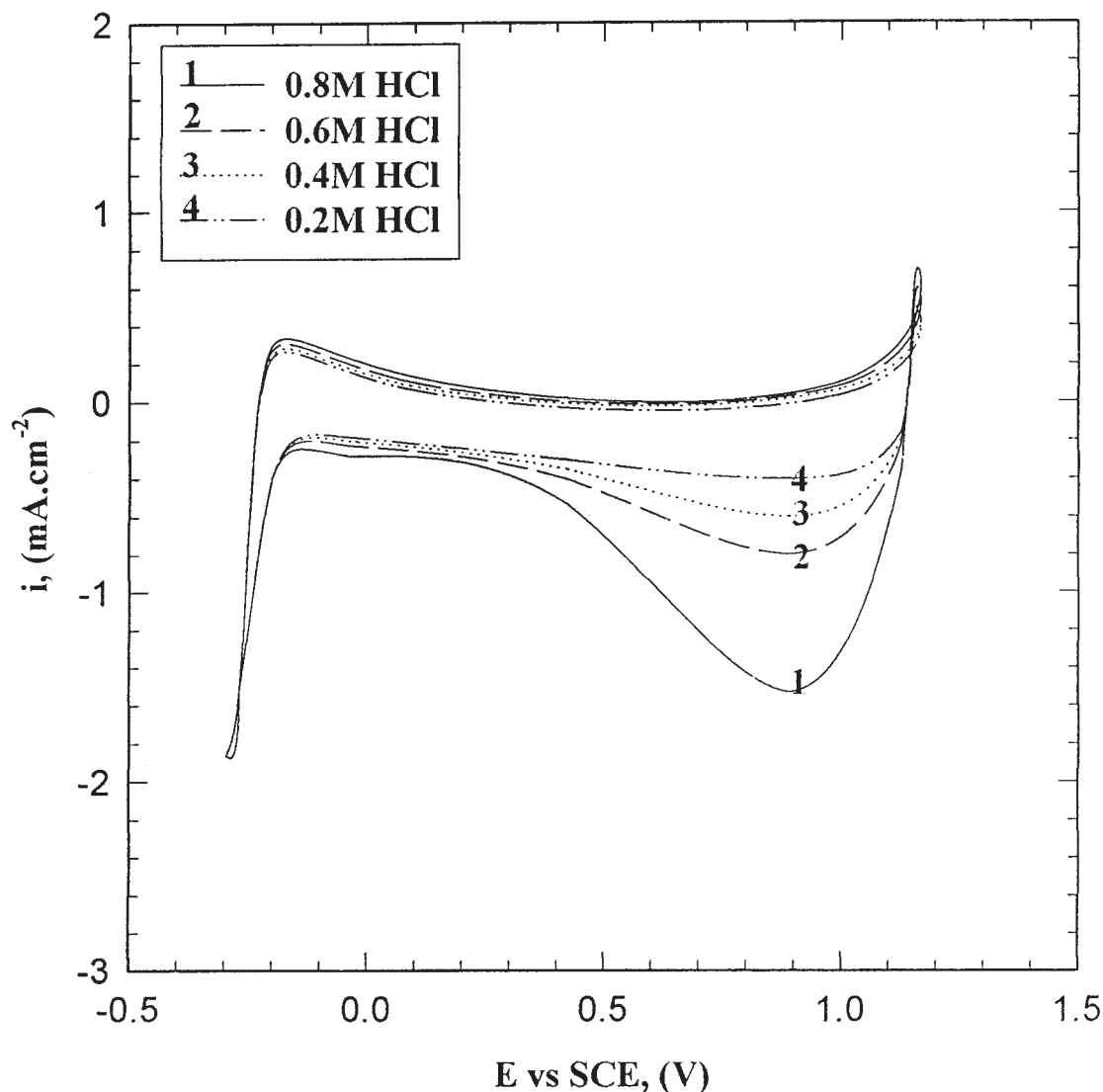


Figure 11 Electrochemical behavior of POAP prepared at its optimum conditions in a free-monomer solution in different HCl concentrations with scan rate 25 mV s^{-1} .

polaron structure (i.e., benzenoid structure) of POAP (cf. Scheme 2). It is also noticed from the voltammogram that the cathodic current peak increases with increasing acid concentration in the range between 0.2 and 0.8 mol/L

Surface morphology

In most conditions, a homogeneous, smooth, brown, and well-adhering POAP films were electrodeposited on the platinum electrode surface. The X-ray diffraction pattern shows that the prepared polymer is a crystalline material as shown in Figure 12(A), for which it is clear that there are two peaks at 2θ angle equal to 20.808 and 23.126.

The surface morphology of the polymer obtained at the optimum conditions was examined by scanning

electron microscopy. The SEM micrograph shows tubular or fibrillar elongated crystals [cf. Figure 12(B)].

CONCLUSIONS

In conclusion, the data obtained reveals the following:

1. The initial rate of electropolymerization reaction of *o*-AP on the platinum electrode is relatively low. The fraction of the dissolved product may be strongly dependent on temperature and monomer or HCl concentrations.
2. The order of electropolymerization reaction of *o*-AP on platinum electrode is 1.125, 1.29, and 0.50, with respect to HCl concentration, monomer concentration, and current density, respectively.

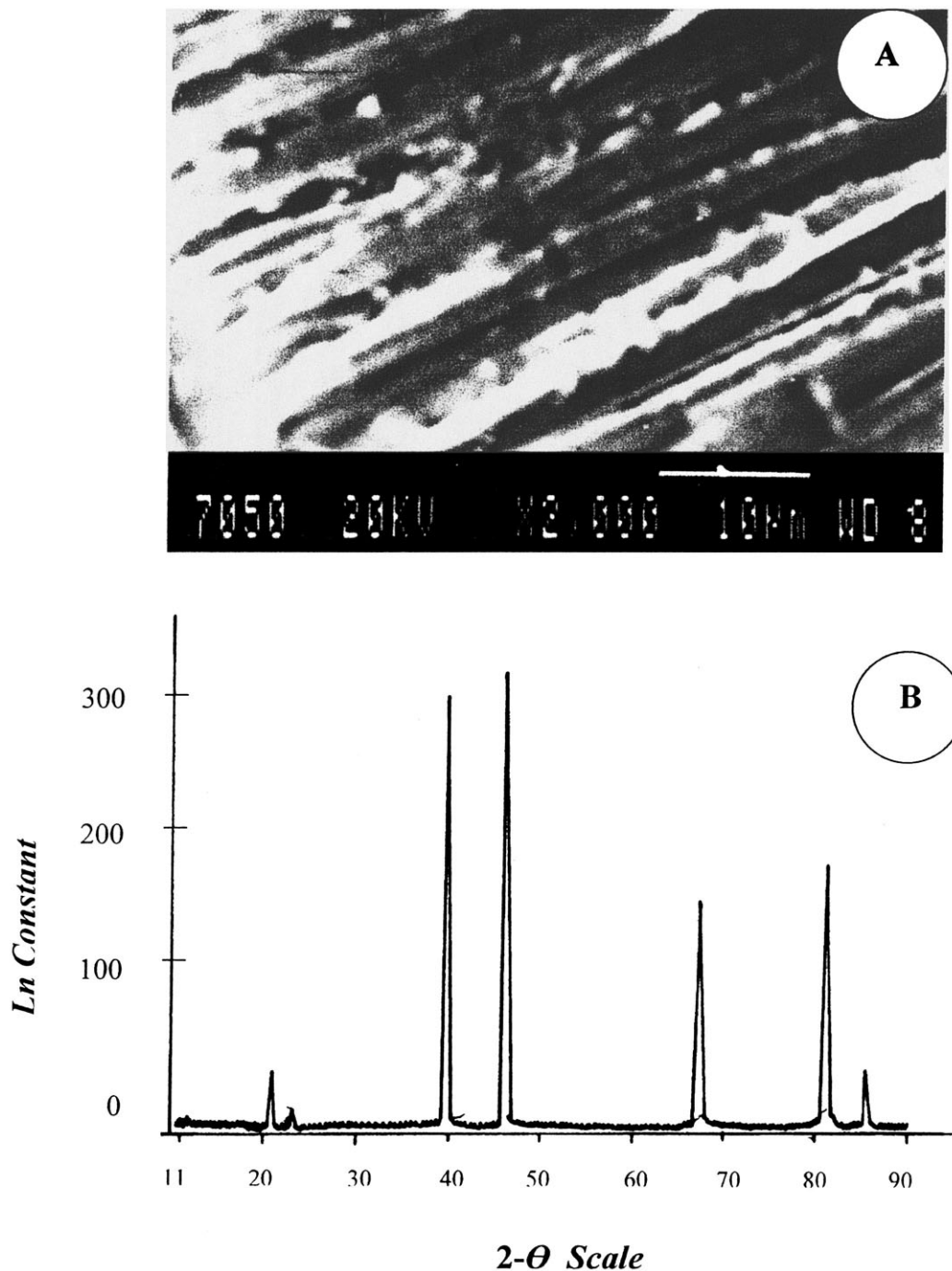


Figure 12 (A) The picture of scanning electron microscope of POAP. (B) X-ray diffraction pattern of POAP.

3. The apparent activation energy is $68.63 \text{ kJ mol}^{-1}$.
4. The prepared POAP is smooth, brown, tubular or fibrillar, crystalline, and well adhered on platinum surface.
5. From cyclic voltammetry studies, it is clear that the cyclic voltammogram consist of two pairs of resolved peaks at -300 and $+810 \text{ mV vs. SCE}$, the first corresponding to the conversion of amine nitrogens to radical cations, and the sec-

ond to the conversion of the radical cations to imine nitrogens. The electroformation of the polymer film on the platinum electrode may be described partially by a diffusion-controlled process.

References

1. Kobayashi, T.; Yoneyama, H.; Tamura, H. *J Electroanal Chem* 1984, 161, 419.

2. Kitani, A.; Kaya, M.; Sasaki, K. *J Electrochem Soc* 1986, 133, 1069.
3. MacDiarmid, A. G.; Yang, L. S.; Hung, W. S.; Humphray, B. D. *Synth Met* 1987, 18, 393.
4. Girard, F.; Ye, S.; Laperriere, G.; Belanger, D. *J Electroanal Chem* 1992, 334, 35.
5. Ye, S.; Girard, F.; Belanger, D. *J Phys Chem* 1993, 97, 12373.
6. Ye, S.; Belanger, D. *J Electrochem Soc* 1994, 141, 149.
7. Nakajima, T.; Kawagoe, T. *Synth Met* 1989, 28C, 629.
8. Geniès, E. G.; Lipkowski, M.; Santier, C.; Viel, E. *Synth Met* 1987, 18, 631.
9. Gottesfeld, S.; Redondo, A.; Feldberg, S. W. *J Electrochem Soc* 1987, 134, 271.
10. Nguyen, M. T.; Deo, L. H. *J Electrochem Soc* 1989, 136, 2131.
11. Paul, E. W.; Ricco, A. J.; Wrighton, M. S. *J Phys Chem* 1985, 89, 1441.
12. Chao, S.; Wrighton, M. S. *J Am Chem Soc* 1987, 109, 6627.
13. Dhaw, S. K.; Trivedi D. C. *Polymer Int* 1991, 25, 55.
14. Joseph, J.; Trivedi, D. C. *J Bull Electrochem* 1992, 22, 563.
15. Thanachasai, S.; Rokutanazono, S.; Yoshida, S.; Watanabe, T. *Anal Sci* 2002, 18, 773.
16. Garcia, M. A. V.; Blanco, B. T.; Ivaska, A. *J Electrochim Acta* 1998, 43, 3533.
17. Nagoaka, T.; Kakuma, K.; Fujimoto, M.; Nakao, H.; Yano, J.; Ogura, K. *J Electroanal Chem* 1994, 369, 315.
18. Anglopoulos, M. *IBM J Res & Dev* 2001, 45, 57.
19. Sathiyarayanan, S. K.; Dhawan, S.; Trivedi, D.C.; Balakrishnan, K. *Corros Sci* 1992, 33, 1934.
20. Sazou, D.; Georgolios, C. *J Electroanal Chem* 1997, 429, 81.
21. Troch-Nagels, G.; Winand, R.; Weymeersch, A.; Renard, L. *J Appl Electrochem* 1992, 22, 756.
22. Bernard, M. C.; Joiret, S.; Hugot-LeGoff, A.; Phong, P. V. *J Electrochem Soc* 2001, 148, 12.
23. Brusic, V.; Anglopoulos, M.; Graham, T. *J Electrochem Soc* 1997, 144, 436.
24. Su, W.; Iroch, O. *J Synth Met* 1998, 95, 159.
25. Dimitra, S.; *Synth Met* 2001, 118, 133.
26. Camalet, J. L.; Lacroix, J. C.; Aeiyaich, S.; Chame-Ching, K.; Lacaze, P. C. *Synth Met* 1998, 93, 133.
27. Kinlen, P. G.; Ding, Y.; Silverman, D. C. *Corrosion* 2002, 58, 490.
28. Lu, W. K.; Elsenbaumer, R. L.; Wessling, B. *Synth Met* 1995, 71, 2136.
29. Shim, Y. B.; Won, M. S.; Park, S. M. *J Electrochem Soc* 1990, 137, 538.
30. Leclerc, M.; Guay, J.; Dao, L. H. *Macromolecules* 1989, 29, 649.
31. Adams, R. N. *Electrochemistry at Solid Electrodes*; Wiley: New York, 1974.
32. Barbero, C.; Silber, J. J.; Sereno, L. *J Electroanal Chem* 1989, 263, 333.
33. Sayyah, S. M.; Bahgat, A. A.; Abd El-Salam, H. M. *Int J Polym Mater* 2002, 61, 291.
34. Prater, K. B. *J Electrochem Soc* 1973, 120, 365.
35. Rach, H. C. *Polym Prepr (Am Chem Soc Div Polym Chem)* 1966, 7, 576.
36. Hernandez, N.; Ortega, J. M.; Choy, M.; Ortiz, R. *J Electroanal Chem* 2001, 515, 123.
37. Barbero, C.; Zerbino, J.; Sereno, L.; Pasado, D. *J Electrochim Acta* 1987, 32, 693.
38. Barbero, C.; Silber, J. J.; Sereno, L. *J Electroanal Chem* 1990, 291, 81.
39. Rodriguez Neto, F. J.; Tucceri, R. I. *J Electroanal Chem* 1996, 416, 1.
40. Ohsaka, T.; Kunimura, S.; Oyama, N. *J Electroanal Chem* 1988, 33, 639.
41. Goncalves, D.; Faria, R. C.; Yonshiro, M.; Bulhões, L. O. S. *J Electroanal Chem* 2000, 487, 90.
42. Komura, T.; Ito, Y.; Yamaguti, T.; Takahasi, K. *J Electrochim Acta* 1998, 43, 723.
43. Tucceri, R. I.; Barbero, C.; Silber, J. J.; Sereno, L.; Posadas, D. *J Electrochim Acta* 1997, 42, 919.
44. Jackowska, K.; Bukowska, J.; Kudelski, A. *J Electroanal Chem* 1993, 350, 177.
45. Sayyah, S. M.; Abd El-Rehim, S. S.; El-Deeb, M. M. *Appl Polym Sci* 2003, 90, 1783.
46. Sayyah, S. M.; Abd El-Rehim, S. S.; El-Deeb, M. M. *Int J Polym Mater* 2004, 53, 1.
47. Sayyah, S. M.; Abd El-Rehim, S. S.; El-Deeb, M. M. *J Appl Polym Sci* 2004, 94, 941.
48. Sayyah, S. M.; Abd El-Rehim, S. S.; Ibrahim, M. A.; Kamal, S. M. *Int J Polym Mater* 2005, 54, 815.
49. Silverstein, R. ; Bassler, C. G.; Morill, T. C. *Spectroscopic Identification of Organic Compounds*; Wiley: New York, 1974.
50. Buzarovska, A.; Arsovo, L.; Arsov, L. *J Serb Chem Soc* 2001, 66, 27.